Review of Selected Features of the Natural System Model, and Suggestions for Applications in South Florida

Water Resources Investigations Report 97-4039

U.S. GEOLOGICAL SURVEY
Prepared in cooperation with the
U.S. Army Corps of Engineers, Jacksonville District

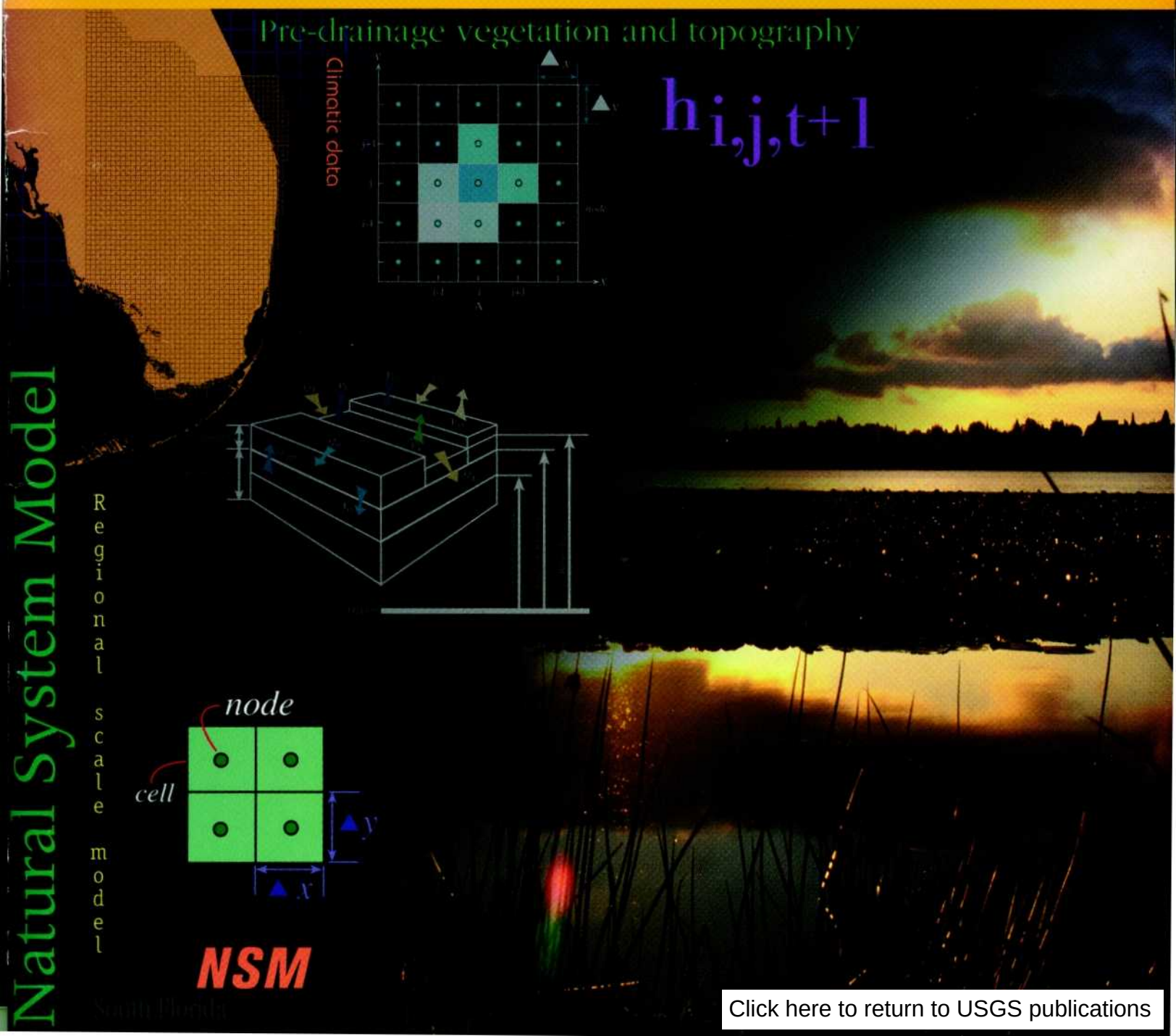

Review of Selected Features of the Natural System Model, and Suggestions for Applications in South Florida

By JERAD D. BALES, JANICE M. FULFORD, and ERIC SWAIN

U.S. GEOLOGICAL SURVEY

Water-Resources Investigations Report 97–4039

Prepared in cooperation with the

U.S. Army Corps of Engineers, Jacksonville District

Raleigh, North Carolina
1997

U.S. DEPARTMENT OF THE INTERIOR
BRUCE BABBITT, Secretary

U.S. GEOLOGICAL SURVEY
Gordon P. Eaton, Director

For additional information write to:

District Chief
U.S. Geological Survey
227 N. Bronough Street, Suite 3015
Tallahassee, FL 32301

Copies of this report can be purchased from:

U.S. Geological Survey
Branch of Information Services
Box 25286, Federal Center
Denver, CO 80225

CONTENTS

Abstract 1
Introduction 2
Purpose and scope 6
Previous investigations 7
Acknowledgments 10
Governing equations and boundary conditions 10
River-system flow equations 11
Overland flow 14
Equations 14
Boundary conditions 20
Ground-water flow 20
Equations 20
Boundary conditions 22
Review of selected features of the Natural System Model 23
Initial and boundary conditions 24
Computational grid size and time step 24
River system 28
Overland-flow system 32
Natural System Model version 4.3 and two-dimensional hydrodynamic model overland-flow simulations 33
Natural System Model version 4.4 34
Conclusions 34
Suggestions for application of the Natural System Model 36
Suggested modifications 36
Appropriate applications 37
Issues for possible future investigation 39
References 39
Appendix—List of variables 41

FIGURES

1.–3. Maps showing:
1. Generalized south Florida land use and hydrology during the early 1900's and the mid-1990's 3
2. Selected management areas of the south Florida watershed 4
3. The Natural System Model grid for south Florida and inset showing relation between nodes and cells 5

4.–8. Diagrams showing:
4. Variables used in the river-system equation. *(A)* Longitudinal view along the length of a river system, and *(B)* Side view of a cell within a river segment 13
5. Intracell and intercell hydrologic processes represented within the Natural System Model 14
6. Overland and ground-water flow variables in the Natural System Model 15
7. Computational modules or active cells in a grid fragment for solution of overland flow between cells for calculations for $H_{i,j,t+1}$ proceeding from *(A)* west to east and north to south, and *(B)* east to west and south to north 16
8. Computational modules or active cells in a grid fragment for the ground-water computations for $h_{i,j,t+1}$ proceeding from *(A)* west to east and sorth to north, and *(B)* east to west and north to south 22

9.–13. Graphs showing:
9. Combined effects of computational cell size and time step on mean ponding depth and mean depth to ground water for a grid velocity of 0.12 foot per second 26

10. Combined effects of computational cell size and time step on mean ponding depth and mean depth to ground water for a grid velocity of about 0.35 foot per second 27
11. Stages computed for eight NSM rivers by using the original NSM river outflow algorithm and a modified algorithm based on the Manning equation 30
12. Jupiter River stage computed by using the original NSM river-system algorithm and a modified river-system algorithm in which there is no coupling between the river and ground-water systems 31
13. Stages computed for four NSM river systems by using the original NSM river-system algorithm and a modified algorithm in which there is no coupling between the overland-flow and river systems 31

TABLES

1. Review issues and approaches for review 7
2. Mean ponding depths and depths to ground water as a function of computational grid size and time step 25
3. Simulated water-level differences, ponding depths, and depths to ground water made by using NSM version 4.3 (2-mile grid, 6-hour time step) and other combinations of grid size and time step for October 1965 conditions 28
4. Summary of tests of river-system algorithms 29
5. Comparison of NSM and TRIM results 33

CONVERSION FACTORS, VERTICAL DATUM, AND ACRONYMS

Multiply	By	To obtain
	Length	
inch (in.)	2.54	centimeter
foot (ft)	0.3048	meter
mile (mi)	1.609	kilometer
	Area	
acre	0.4047	hectare
square mile (mi^2)	2.590	square kilometer
	Flow	
foot per second (ft/s)	0.3048	meter per second
cubic foot per second (ft^3/s)	0.02832	cubic meter per second

Sea level: In this report "sea level" refers to the National Geodetic Vertical Datum of 1929 (NGVD of 1929)—A geodetic datum derived from a general adjustment of the first-order level nets of both the United States and Canada, formerly called Sea Level Datum of 1929.

Acronyms:

EAA	Everglades Agricultural Area
ENP	Everglades National Park
LEC	Lower East Coast
NSM	Natural System Model
RMS	root mean square
SFWMD	South Florida Water Management District
SFWMM	South Florida Water Management Model
TRIM	tidal residual, intertidal mudflat
USGS	U.S. Geological Survey
WCA	Water Conservation Area

Review of Selected Features of the Natural System Model, and Suggestions for Applications in South Florida

By Jerad D. Bales, Janice M. Fulford, *and* Eric Swain

ABSTRACT

A study was conducted to review selected features of the Natural System Model, version 4.3. The Natural System Model is a regional-scale model that uses recent climatic data and estimates of historic vegetation and topography to simulate pre-canal-drainage hydrologic response in south Florida. Equations used to represent the hydrologic system and the numerical solution of these equations in the model were documented and reviewed. Convergence testing was performed using 1965 input data, and selected other aspects of the model were evaluated.

Some conclusions from the evaluation of the Natural System Model include the following observations. Simulations were generally insensitive to the temporal resolution used in the model. However, reduction of the computational cell size from 2-mile by 2-mile to 2/3-mile by 2/3-mile resulted in a decrease in spatial mean ponding depths for October of 0.35 foot for a 3-hour time step.

Review of the computer code indicated that there is no limit on the amount of water that can be transferred from the river system to the overland-flow system, on the amount of seepage from the river to the ground-water system, on evaporation from the river system, or on evapotranspiration from the overland-flow system. Oscillations of 0.2 foot or less in simulated river stage were identified and attributed to a volume limiting function which is applied in solution of the overland-flow equations. The computation of the resistance coefficient is not consistent with the computation of overland-flow velocity. Ground-water boundary conditions do not always ensure a no-flow condition at the boundary. These inconsistencies had varying degrees of effects on model simulations, and it is likely that simulations longer than 1 year are needed to fully identify effects. However, inconsistencies in model formulations should not be ignored, even if the effects of such errors on model results appear to be small or have not been clearly defined.

The Natural System Model can be a very useful tool for estimating pre-drainage hydrologic response in south Florida. The model includes all of the important physical processes needed to simulate a water balance. With a few exceptions, these hydrologic processes are represented in a reasonable manner using empirical, semi-empirical, and mechanistic relations. The data sets that have been assembled to represent physical features, and hydrologic and meteorological conditions are quite extensive in their scope.

Some suggestions for model application were made. Simulation results from the Natural System Model need to be interpreted on a regional basis, rather than cell by cell. The available evidence suggests that simulated water levels should be interpreted with about a plus or minus 1 foot uncertainty. It is probably not appropriate to use the Natural System Model to estimate pre-drainage discharges (as opposed to hydroperiods and water levels) at a particular location or across a set of adjacent computational cells. All simulated results for computational cells within about 10 miles of the

model boundaries have a higher degree of uncertainty than results for the interior of the model domain. It is most appropriate to interpret the Natural System Model simulation results in connection with other available information. Stronger linkages between hydrologic inputs to the Everglades and the ecological response of the system would enhance restoration efforts.

INTRODUCTION

The south Florida ecosystem has been greatly altered during the last 100 years (fig. 1). Drainage of the south Florida watershed began in the early 1880's, and by the early 1990's about 50 percent of the historic Everglades had been drained by ditches and canals. In response to flooding and to provide water for a variety of human uses, a complex water-management system that includes levees, well fields, pumps, canals, and control structures was constructed throughout south Florida. This system provides a steady supply of freshwater to a growing population of more than 4 million people in the Lower East Coast (LEC) Water Supply Plan service areas; to agricultural areas primarily in the Everglades agricultural area (EAA) and east of the Everglades National Park (ENP); to the Big Cypress National Preserve; and to the ENP and subsequently Florida Bay (fig. 2).

The South Florida Water Management Model (SFWMM) was developed by the South Florida Water Management District (SFWMD) in the late 1970's and early 1980's to simulate the hydrology of this water-management system in south Florida (MacVicar and others, 1984). The SFWMM is a regional model that includes simulation of hydrologic processes (evapotranspiration, surface flow, infiltration, ground-water flow, canal flow, and canal-aquifer interactions) and water-management activities (canal stage maintenance, water-control structure operation, and water withdrawals) in an approximately 7,600-square-mile (mi^2) area. The effects of water-management scenarios on time-varying ground- and surface-water conditions and on canal flows are simulated for selected static land uses and management schemes. Time-varying historic rainfall and evapotranspiration data from 1965 to 1990, actual or predicted ground-water withdrawals, and irrigation demands for the LEC areas are used as model inputs for the simulations. The model is calibrated using time-series ground- and surface-water-level data collected from more than 100 monitoring stations in the modeled area.

The Natural System Model (NSM) simulates the hydrologic response of pre-canal-drainage south Florida by using 1965–90 climatic data and estimated physical features of the modeled region. The NSM was developed directly from the SFWMM by the SFWMD in about 1989 and was established as version 3.4 (Perkins and MacVicar, 1991). Following a review (Fennema, 1992), modifications were made by the SFWMD and version 3.6 was established, and limited documentation was published (Fennema and others, 1994). The NSM has been undergoing more or less continuous updates since that time, and changes have been documented primarily in SFWMD memoranda and internal reports.

The NSM uses the same climatic input data and model parameters, and similar model algorithms and computational schemes as the SFWMM. However, to simulate the hydrologic response of the natural system, SFWMM physical features, such as topography, vegetation, land use, and hydromodifications, have been adjusted to represent pre-drainage conditions. The vegetation coverage for the NSM was derived from a landscape map of south Florida for the early 1900's, and pre-drainage channels or rivers were identified from surveys completed between 1855 and 1870. The NSM topography is generally the same as that used in the SFWMM, except in areas of known soil subsidence.

Overland flow is the dominant water-transport mechanism in the natural system, whereas ground-water and canal flows dominate in the managed, or existing system. Significant overland flows do occur in the natural areas, such as the ENP, of the SFWMM domain. In addition to overland flow, processes included in the NSM are rainfall, evapotranspiration, infiltration, ground-water flow, and flows in some small, coastal rivers (fig. 3). Inflows to Lake Okeechobee include estimated "natural" river inflows, overland flow, ground-water flow, and rainfall. Outflows from the lake to south Florida occur when the lake stage exceeds the estimated land-surface elevation of the southern rim of the lake.

The NSM domain covers an area of about 9,312 mi^2 (fig. 3) and consists of 2,328 computational cells, 2-mile (mi) by 2-mi each. Water level, velocity, land elevation, vegetation, and land use are assumed to be uniform within each cell, and flow may enter or exit the cell along any of the four sides. Rather than modeling

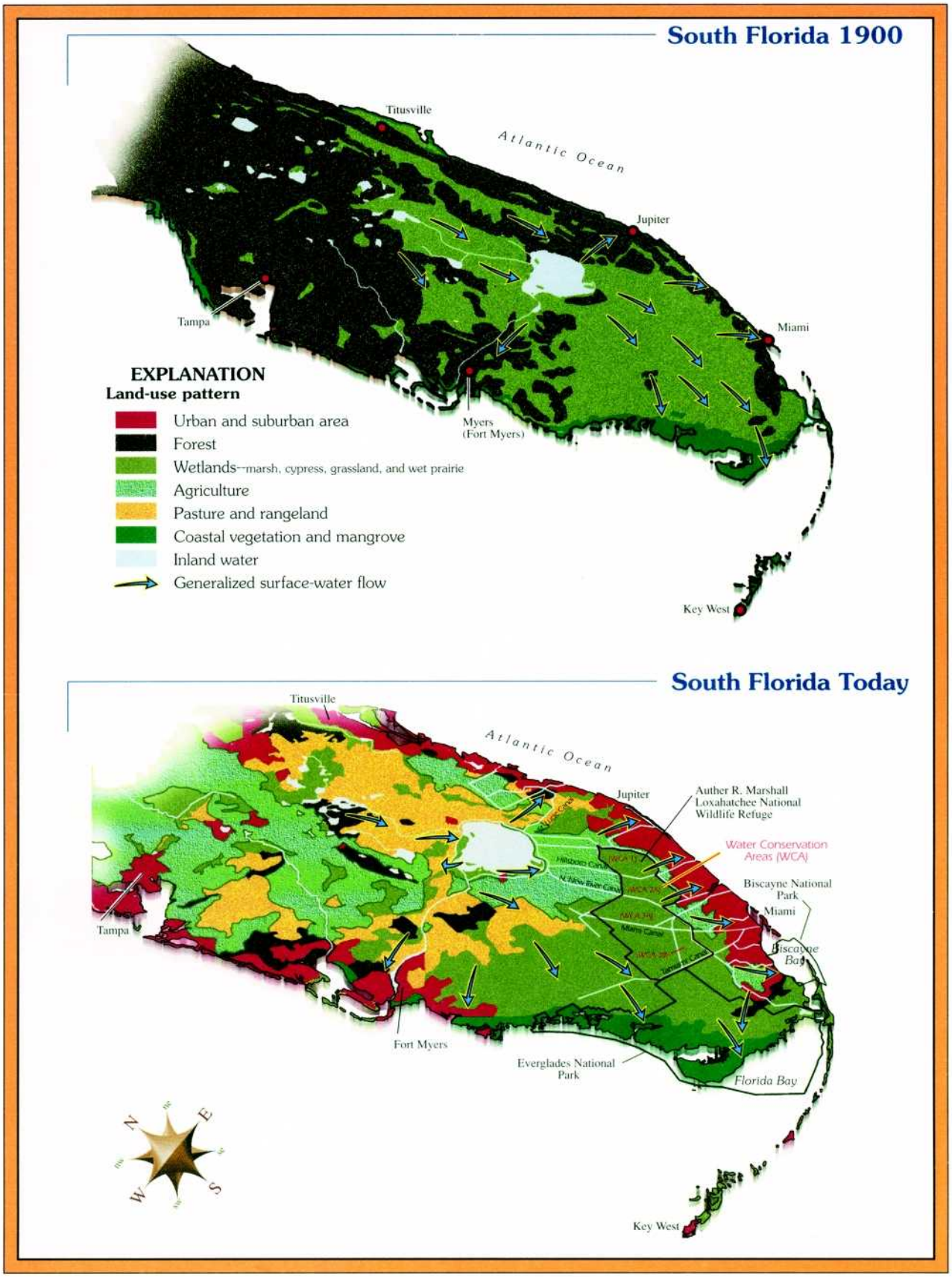

Figure 1. Generalized south Florida land use and hydrology during the early 1900's and the mid-1990's.

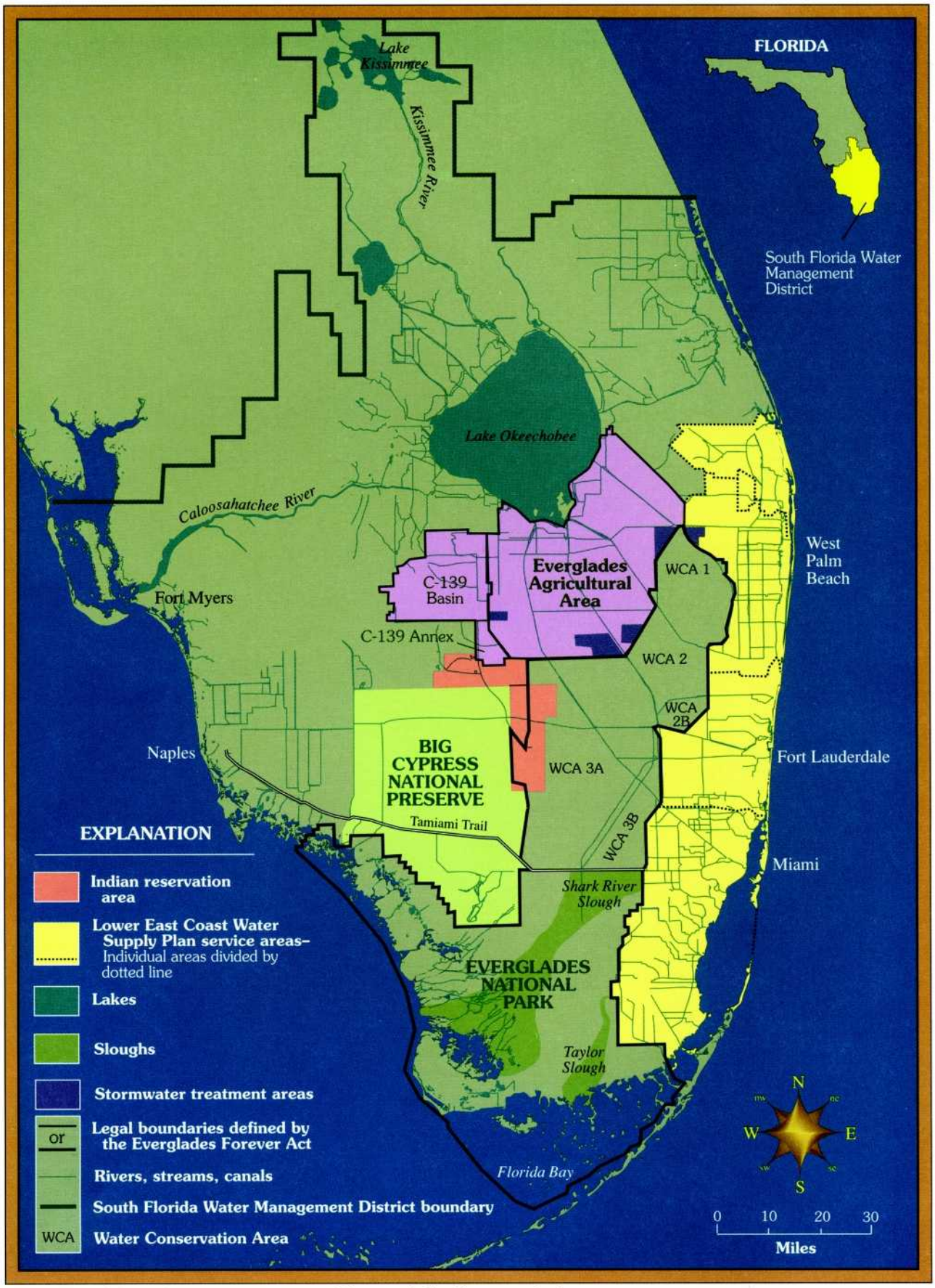

Figure 2. Selected management areas of the south Florida watershed.

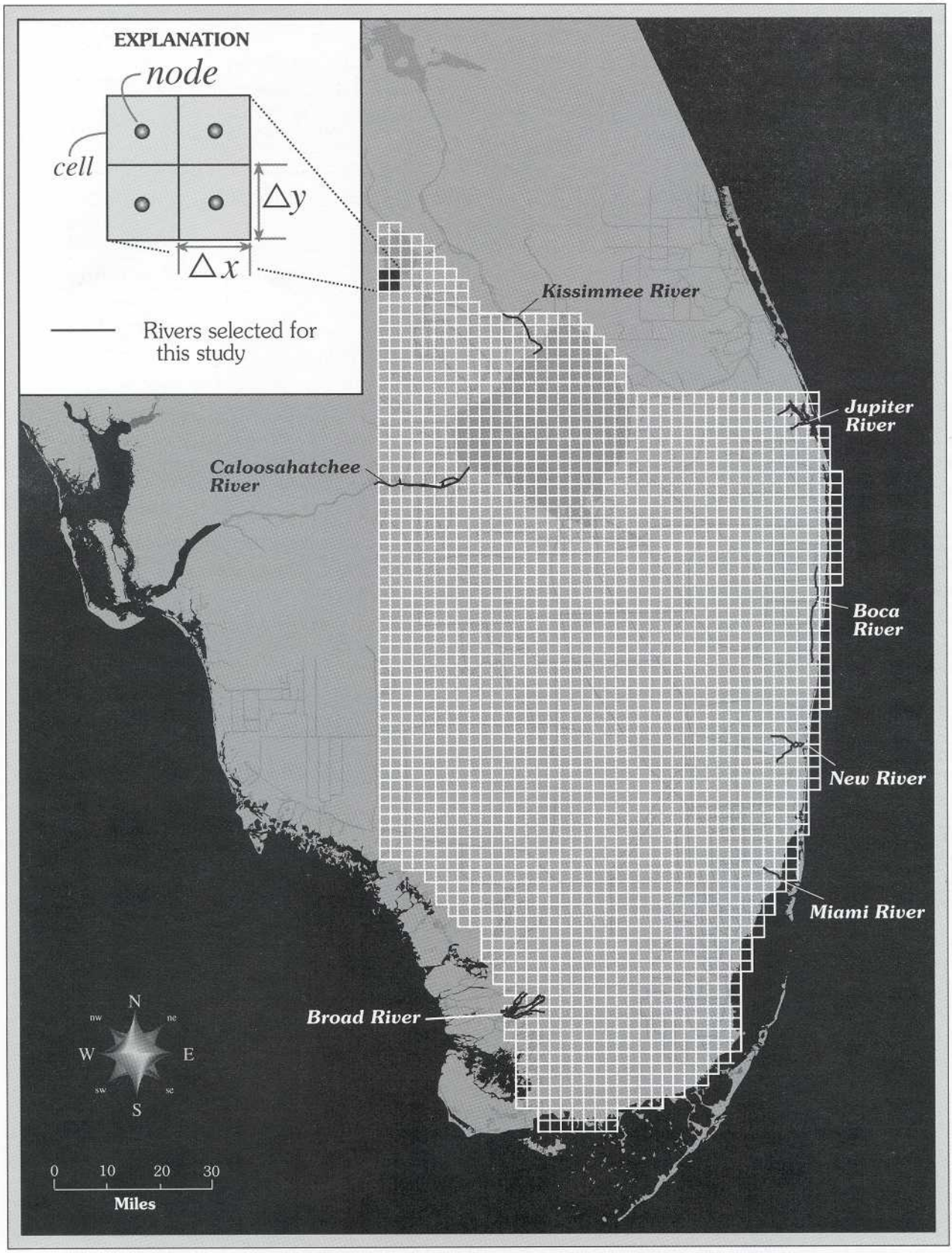

Figure 3. The Natural System Model grid for south Florida and inset showing relation between nodes and cells.

all physical processes explicitly (such as the complete three-dimensional turbulent flow, and the heat and water transport associated with evapotranspiration), the NSM includes several parameters which are used to simplify descriptions of these complex processes.

The NSM is somewhat unique in that the model is fundamentally linked to the SFWMM. Model parameters for the NSM are obtained from the calibrated SFWMM, because the NSM cannot be calibrated directly. This means that if the SFWMM is modified and subsequently recalibrated, then model parameters in the NSM also must be changed and new NSM simulations made. Moreover, algorithms describing hydrologic processes in the two models must be the same in order for model parameters in the NSM to have the same meaning in the NSM as in the calibrated SFWMM. Consequently, it is generally true that changes in either the NSM or the SFWMM must be accompanied by changes in the other model, followed by a new calibration of the SFWMM.

The accuracy and validity of the NSM cannot be tested using traditional modeling approaches because hydrologic data from the pre-drainage south Florida ecosystem do not exist for comparison with model results. Moreover, accurate, detailed information on historic vegetative and topographic conditions required for the NSM simulations is largely unavailable, leading to additional uncertainty in model output. Calibrated model parameters from the SFWMM are transferred directly to the NSM, but these parameters may represent different processes in the two models for some parts of the model domain, particularly where there have been changes in land use, topography, vegetation, and drainage patterns.

In the past, the performance of the NSM was evaluated by using three approaches. First, because the fundamental algorithms used in the NSM are the same as those used in the SFWMM, and because the SFWMM appears to perform adequately, it was assumed that the NSM properly simulates the important hydrologic processes. Second, a series of tests was performed by the SFWMD to identify (1) the sensitivity of the NSM simulations to changes in selected model parameters and (2) geographic areas in which the simulated hydrology is most sensitive to changes in model parameters. Third, results from the NSM were compared with available, but somewhat limited, historic information, on soils and vegetation.

A major, interagency effort is underway to restore significant portions of the south Florida ecosystem and to enhance the quantity, quality, and timing of freshwater flows to the remaining Everglades. A key component of this restoration effort involves identifying hydropattern targets (primarily frequency, duration, depth, and spatial extent of water inundation) at selected key locations in the Everglades. The NSM has been proposed as the "best available tool" for estimating hydropattern targets for restoration efforts. Restoration costs may be nearly $2 billion, and decisions made based on NSM results could have important and direct implications for the entire south Florida region.

The U.S. Geological Survey (USGS), in cooperation with the U.S. Army Corps of Engineers, Jacksonville District, conducted a study to review selected features of the NSM to determine if the NSM can provide a reasonable simulation of south Florida hydrology for pre-drainage conditions using recent climatic data. The absence of measured hydrologic, topographic, and vegetation data from the natural system for model construction and testing required that non-standard procedures be used to determine if NSM results are "reasonable." Only selected components and features of the model were reviewed because of limited resources and time available for the review. Issues identified during discussions with staff from the SFWMD, U.S. Army Corps of Engineers, National Park Service, and Florida Department of Environmental Protection were the focus of the review, and subsequently this report (table 1).

Purpose and Scope

The purpose of this report is to document a review of selected features of the Natural System Model. Equations used to represent various components of the natural hydrologic system, along with numerical schemes used to solve the equations, were reviewed in order to clearly describe and document the manner in which processes were modeled. The effects of different temporal and spatial discretizations on model results were evaluated, and sensitivity tests were conducted using selected algorithms. Suggestions are made for appropriate uses of the NSM, based on findings from this review.

The SFWMD provided the USGS with NSM version 4.3, which was evaluated during the study by using the 1965 climatic data set also provided by the SFWMD. However, as a result of preliminary findings

Table 1. Review issues and approaches for review

Issue	Review approach
Spatial and temporal discretization.	Comparison of model results made using different computational grid cell sizes and time steps.
Spatial interpolation of precipitation data.	Review of literature and model algorithms.
Evapotranspiration computations.	Review of literature and model algorithms.
River system algorithms.	Review of governing equations, numerical solution of the equations, and model algorithms; sensitivity tests.
Overland flow algorithms.	Review of governing equations, numerical solution of the equations, and model algorithms; comparison of NSM approach with other approaches.
Ground-water system algorithms.	Review of governing equations, numerical solution of the equations, and model algorithms.
Initial and boundary conditions.	Limited review of data; review of model algorithms.
Recommended applications.	Synthesis of available information and results from reviews.

during the course of this study, revisions were made by the SFWMD to version 4.3, resulting in version 4.4. Subsequent changes may have been made in response to findings reported herein.

Previous Investigations

The primary documentation of the NSM was published by Fennema and others (1994). The report provides an overview of NSM version 3.6; an analysis of the sensitivity of model results to changes in evapotranspiration, the overland-flow resistance coefficient, and Lake Okeechobee water levels; and a comparison of NSM results to data and SFWMM simulation results. Documentation of governing equations, solution techniques, selection of model parameters, and input data were not provided. One of the first versions of the SFWMM, from which the NSM was developed, was documented by MacVicar and others (1984). Since that time, the SFWMM has undergone numerous revisions.

Water levels and inundation periods in Water Conservation Area (WCA) 1 (fig. 2) were fairly insensitive to changes in evapotranspiration (Fennema and others, 1994). However, water levels and inundation periods in WCA 3A and at the northern end of Shark River Slough (fig. 2) were sensitive to changes in evapotranspiration. A 20-percent reduction in evapotranspiration resulted in a 73-percent increase in annual flow into Shark River Slough, and a 20-percent increase in evapotranspiration resulted in a 60-percent decrease in annual flow into the slough.

Water levels and inundation periods were generally insensitive to changes in the resistance coefficient and Lake Okeechobee water levels (Fennema and others, 1994). Flows, however, were sensitive to changes in the resistance coefficient, particularly during drier years. Flows as far south as Tamiami Trail were sensitive to changes in Lake Okeechobee water levels, with an increase of 1.5 feet (ft) in the mean lake water level resulting in 34 percent more flow at Tamiami Trail. Similar analyses for later versions of the NSM have been performed by the SFWMD staff, but have not been published, so it is not known if these results remain valid for the current version of the NSM.

Simulated water levels for the period 1980–89 were compared with measured water levels at several locations (Fennema and others, 1994). Simulated water levels and measured water levels in WCA 1 (fig. 2) exhibited fairly similar temporal patterns and differed by less than 1 ft in most months. The water-level gage in WCA 1 is in the Loxahatchee National Wildlife Refuge, which is somewhat less affected by water management activities than many other locations in south Florida. Simulated and measured water levels in the ENP also had very similar seasonal patterns, and differences between simulated and measured water levels were generally less than a foot in the western Shark River Slough and in the downstream portion of Taylor Slough (fig. 2). These results, while not a calibration of the NSM, suggest that reasonable temporal water-level patterns are simulated by the NSM in selected regions of the model domain.

Because of the absence of pre-drainage hydrologic data, the NSM simulations were qualitatively compared with available historic information to obtain a "quasi-validation" of the model.

Preliminary results (J. Obeysekera, South Florida Water Management District, written commun., August 1996) indicate that (1) simulated flow patterns are consistent with known flow patterns in the Everglades, (2) the simulated extent of inundation generally agrees with the known historic extent of the Everglades, (3) the largest simulated ground-water fluxes are to the east, consistent with historic accounts of large gradients near the Atlantic coast, and (4) simulated Lake Okeechobee levels seem to agree, in general, with historic accounts of lake levels and overflows.

An extensive analysis of historic data on soils, water depths, vegetation, and other information was conducted to reconstruct the spatial pattern of long-term average water levels and hydroperiods in south Florida for the pre-drainage period (C. McVoy, Environmental Defense Fund, written commun., 1997). The reconstructed water levels and hydroperiods were compared with simulations made using NSM version 4.4. Spatial patterns of water levels and hydroperiods from the two sets of records were in general agreement. However, long-term average annual low and high water levels simulated by the NSM were generally lower than those estimated from the historic records, with differences ranging up to 18 inches (in.). Likewise, the annual range in simulated water levels was less than the range estimated from historic records, with a simulated range of about 1 ft and a range estimated from historic records of 2 ft. Available historic records were insufficient for estimating pre-drainage flow volumes. Interannual variations in high and low water levels were not determined, but limited information indicated that variations of up to 1 ft around the long-term average might have been common. It is important to note, however, that soils and, to a lesser extent, vegetation integrate the effects of centuries of climatic and hydrologic variability, whereas NSM version 4.4 simulates pre-drainage hydrologic response based on about 25 years of recent climatic data.

Loucks and Stedinger (1994) addressed the issues of sensitivity analysis and uncertainty in the SFWMM and the NSM. The variability and uncertainty in model output was determined to be a function of model inputs, parameter values, initial and boundary conditions, and model structure, including numerical solution techniques. Loucks and Stedinger noted that parameter and model uncertainties become more important when the model is used to extrapolate beyond conditions that have been observed. Several recommendations were made concerning approaches for conducting sensitivity and uncertainty analyses for the SFWMM and the NSM. Loucks and Stedinger also recommended that automated model calibration routines be developed for objective model calibration and better determination of statistical properties of model parameters.

In response to the report by Loucks and Stedinger (1994), Trimble (1995) conducted an investigation to (1) identify the most feasible methods for evaluating the sensitivity of and uncertainty in the SFWMM and (2) apply one or more of the methods to estimate uncertainty associated with selected SFWMM performance measures. Although Trimble's study addressed the SFWMM, results from the investigation are relevant to the NSM because the NSM parameters are derived from the SFWMM calibrations. Trimble noted that, "only a small amount of information exists documenting the reasonable ranges for several [SFWMM] parameters."

Trimble (1995) concluded that there was no region of the model domain which was insensitive to changes in at least one of the model parameters. Potential evapotranspiration dominates all other processes, and evapotranspiration parameters cannot be changed more than 5 percent without degrading the model calibration. Changes in evapotranspiration resulting from parameter adjustments appeared to be balanced by changes in flow.

Water levels in all regions of the model except the ENP, where overland flow is the dominant flow process, were insensitive to changes in the Manning n. Trimble (1995) suggested that use of the Manning relation (which relates water velocity to flow resistance, channel geometry, and channel slope) might not be acceptable for simulating overland flow for 2-mi by 2-mi computational cells in which secondary flow channels are present, and in which significant water-level differences can occur, particularly near the east coast. (Canals are not present in the NSM.) However, Trimble noted that because the SFWMM is used as a water-balance model rather than a flow-routing model, application of the Manning relation may be acceptable.

Trimble (1995) concluded that model parameter uncertainty in the SFWMM is much less than the total uncertainty in the model. Much of the model

uncertainty, according to Trimble, can be associated with rainfall amounts and flows at control structures.

Additional sensitivity analyses were performed by SFWMD staff (J. Obeysekera, South Florida Water Management District, written commun., January 1995). The evapotranspiration crop coefficients and Manning *n*-values were varied, and NSM results were analyzed using a sensitivity matrix. Simulated results were most sensitive to changes in evapotranspiration coefficients and less sensitive to changes in the resistance coefficient. Similar results were reported by Fennema and others (1994). Results were most sensitive to changes in evapotranspiration coefficients in the central region of the model domain (A.M.W. Lal, South Florida Water Management District, written commun., January 1997). A change of 1 ft in the topographic elevation at the southern rim of Lake Okeechobee had a significant effect on simulated flows in the model domain. A change in the evapotranspiration coefficient in one computational cell was found to affect simulated results for a distance of about 5 cells away from the cell in which the change was made.

The simulated flow patterns presented by Fennema and others (1994) exhibited some unusual features. Specifically, velocities along the western boundary of the model were significantly greater than those just to the east of the boundary (fig. 3). Likewise, there was a region of high velocities near the northern boundary of the model domain. Flows at the boundaries were generally parallel to the boundary, and were to the east at the northern boundary and to the south at the western boundary. These flow patterns were not discussed in the report. Similar results were seen in NSM version 4.2 simulations (J. Obeysekera, South Florida Water Management District, written commun., January 1995).

Van Lent and others (1993) used NSM version 3.6 to compare pre- and post-drainage flows in the lower Taylor Slough Basin (fig. 2). The authors noted that the 2-mi by 2-mi computational grid size limited the usefulness of NSM results in small regions, such as Taylor Slough. Additional uncertainty in the Taylor Slough simulations was introduced by the proximity of Taylor Slough to the model boundary, where boundary conditions are estimated. Among the recommendations of Van Lent and others, it was noted that water levels, rather than flows, are the key indicator of marsh restoration.

Van Lent (1995) developed a linear stochastic model for relating water levels in Shark River Slough (fig. 2) to rainfall and potential evapotranspiration. Rainfall alone was found to be a reasonable predictor of Shark River Slough water levels, but the linear model appeared to inadequately replicate the inundation patterns in the slough. Van Lent also concluded that wet season and dry season water-level fluctuations in the Shark River Slough are controlled by different physical processes.

A two-dimensional hydrodynamic model was developed for a 3,815-acre Stormwater Treatment Area (STA) located in the northwest corner of WCA 1 (fig. 2) (Guardo and Tomasello, 1995). The STA is about the size of 1.5 NSM computational cells. Vegetation in the model domain is primarily cattails, mixed macrophytes, submerged macrophytes and algae; this vegetation is like vegetation in much of the NSM domain. The model consisted of 600 computational cells, 600 ft by 906 ft. A Manning formulation was used to describe flow resistance; the Manning *n*-value was set to 1.0 in the model. Simulated flow velocities ranged from 0.0012 to 0.015 foot per second (ft/s) for inflows ranging from 75 cubic feet per second (ft^3/s) to 600 ft^3/s. Manning *n*-values in the NSM range from about 0.04 to more than 2.0, depending on vegetation type and water depth. These differences in Manning *n*-values demonstrate the effects of grid size and model formulation on the *n*-value used in a particular model.

Abtew and others (1993) evaluated six methods for estimating point and areal rainfall in a 4,000-mi^2 area of inland south Florida where 25 raingages were located. The optimal interpolation and kriging methods provided good estimates of monthly point and areal rainfall throughout the study area. In contrast, the NSM daily rainfall in ungaged computational cells (cells representing areas where no raingage is present) is assumed to be equal to the measured rainfall at the nearest raingage. This approach can lead to discontinuities in rainfall when two adjacent computational cells obtain rainfall estimates from two different raingages. In addition, most of the 485 raingages from which the NSM data are obtained are concentrated along the east coast of south Florida. Annual average rainfall in the model domain ranges from about 35 to 65 in., with higher values occurring primarily along the east coast.

Chin and Zhao (1995) used global error variance to, among other things, identify the best method for

estimating reference-crop evapotranspiration (evapotranspiration from a vegetative surface) in south Florida. Global error variance was estimated from evaporation-pan networks and empirical evaporation equations (Penman-Monteith, Blaney-Criddle, and Stephens-Stewart) based on meteorological data-collection networks in the SFWMD, which roughly coincide with the NSM domain. Chin and Zhao concluded that universal kriging provided better estimates of reference-crop evapotranspiration in south Florida than the three empirical equations. They attributed this to the fact that accurate measurements of meteorological parameters, which are required for the empirical equations, are generally unavailable and must be estimated from remote meteorological stations. Of the three empirical functions evaluated, the Penman-Monteith function was found to provide the best estimates of reference-crop evapotranspiration in south Florida. The Penman-Monteith method is used for estimating reference evapotranspiration in the NSM, and an inverse-distance weighting scheme is used for the spatial distribution of the evapotranspiration values.

Bidlake and others (1993) evaluated three micrometeorological methods for estimating evapotranspiration from dry prairies, marshes, pine flatwoods, and cypress swamps in west central Florida. Calculated annual evapotranspiration values during the study period were 39.8 in. (dry prairie), 39.0 in. (marsh), 41.7 in. (pine flatwoods), and 38.2 in. (cypress swamp). Bidlake and others found that evapotranspiration was about 57 percent of potential evapotranspiration at the marsh site. Potential evapotranspiration calculation methods, such as the Penman-Monteith method, were found to be unsuitable for estimating evapotranspiration from pine flatwood and cypress swamp sites. However, potential evapotranspiration methods might be appropriate for marsh vegetation.

Potential evapotranspiration varied seasonally (Bidlake and others, 1993). The 3 months of lowest average potential evapotranspiration at the dry prairie sites were November, December, and January, and the highest potential evapotranspiration was during March through June. Similar seasonal variations likely occurred for the other vegetation types.

Acknowledgments

The assistance, technical guidance, and open discussions provided by M. Choate, U.S. Army Corps of Engineers, Jacksonville District; A. Lal, C. Neidrauer, J. Obeysekera, and R. Van Zee, South Florida Water Management District; and R. Fennema, Everglades National Park, are gratefully acknowledged. E. Hayter, Clemson University, ably performed the comparison of NSM results with simulations from a two-dimensional hydrodynamic model. L. DeLong, U.S. Geological Survey (retired), contributed to the initiation and planning of this investigation.

GOVERNING EQUATIONS AND BOUNDARY CONDITIONS

The basic equation solved by the NSM is conservation of mass. This equation can be expressed as a summation of the changes in volume of the various hydrologic systems as

$$\frac{\partial V_T}{\partial t} = \frac{\partial V_r}{\partial t} + \frac{\partial V_o}{\partial t} + \frac{\partial V_{gw}}{\partial t}, \quad (1)$$

where

V_T is the total water volume in the NSM,
V_r is the water volume associated with the river systems,
V_o is the water volume associated with the overland-flow system,
V_{gw} is the water volume associated with the ground-water system, and
t is time.

Because the surface areas of each system (river, overland flow, and ground-water flow, respectively) are considered constant, equation 1 can be expressed as

$$\frac{\partial V_T}{\partial t} = A_r \frac{\partial Y_r}{\partial t} + A_o \frac{\partial H}{\partial t} + A_{gw} \frac{\partial h}{\partial t}, \quad (2)$$

where

Y_r is the river stage or water-surface elevation for the river system,
H is the overland-flow ponding depth,
h is the ground-water elevation relative to an arbitrary datum, and
A_r, A_o, and A_{gw} are the surface areas of the river, overland-flow, and ground-water systems, respectively.

Equation 2 is a relatively simple partial differential equation. However, each term on the right side of the equation represents a complex hydrologic system, requiring the use of additional equations to compute the values for each of these terms. The following three sections present, in detail, the equations solved by the NSM that represent each of the hydrologic systems—river, overland flow, and ground water—described by the terms on the right side of equation 2.

The partial differential equations are solved in the NSM by using finite-difference techniques. Finite-difference techniques require the subdivision of the solution domain into a grid with a finite number of node points. Continuous derivatives at each point are then replaced by a finite-difference approximation to the derivative. The NSM uses a 41- by 80-node grid to represent the solution domain (fig. 3). Each node represents a 2-mi by 2-mi cell (fig. 3) and is assigned a particular land-use type which reflects the general vegetation, soil type, and flow roughness in the cell. Equations that represent the hydrologic system are then solved for each node and associated cell.

The hydrologic processes that are included within each cell in the NSM, or the intracell hydrologic processes, are precipitation, evapotranspiration, seepage or recharge between the river and ground-water systems, seepage or infiltration from the overland-flow system to the ground-water system, flow from the ground-water system to the overland-flow system, and flow between the overland and river systems. The hydrologic processes represented between cells are ground-water, overland, and river flow. These processes are represented in the governing equations described in the following sections. The effects on flow of solar heating, inertia, rotation of the Earth, and wind are considered negligible for this system and are not included in the governing equations.

For each computational time step, the order of solution is (1) the river system, (2) the overland-flow system, and (3) the ground-water system. Prior to the solution of the river system, precipitation is added to the ponding depths at each node and to river stage throughout the grid. After the solution of the ground-water system, the water-surface elevations in nodes that represent lake land-use types are equalized so that the water-surface elevations are the same for each lake node, resulting in a level lake surface.

River-System Flow Equations

The NSM uses a simplified flow equation to represent river systems. River properties for the appropriate river segment, such as flow length and surface area, are assigned to a node if a river segment lies within the domain of the node (or cell). The equation solved for each river system is

$$\frac{\partial V_r}{\partial t} = Q_f + R_r - Q_r + P_r - E_r, \qquad (3)$$

where

V_r is the volume of water in a river,
Q_f is flow between the river system and the overland-flow system,
R_r is the flow between the river system and the ground-water system (or seepage),
Q_r is the flow into and out of the ends of the river segment in the cell,
P_r is the precipitation directly on the river, and
E_r is evaporation from the river.

This solution technique is similar to storage routing techniques described in many hydrology texts (for example, Linsley and others, 1975). Twenty-nine distinct river systems are included in the NSM domain.

Equation 3 is expressed for each river system as a forward-in-time finite-difference formulation:

$$A_r Y_{t+1} = A_r Y_t + (Q_f + R_r - Q_r - E_r)\Delta t, \qquad (4)$$

where V_r is replaced by the product of the surface area of the individual river system, A_r, and the stage, Y; Y_r is replaced by Y for clarity; and the subscripts t and $t+1$ refer to the present and subsequent computational time steps, respectively. Precipitation is implicit in equation 4 because it is added to the river stage prior to the solution of equation 4. Because the terms on the right side of equation 4 are dependent on Y_{t+1}, an iterative method similar to the bisection technique (Conte, 1980) is used to solve the equation.

The intracell flow between a river and the overland system is computed as

$$Q_f = \sum_{m=1}^{M} \frac{1.49}{n_m}\left[\left|(H_{m,t} + Z_m) - (Y_{t+1} + f_m)\right| \frac{4}{\Delta x}\right]^{\frac{1}{2}} \times \left(\Gamma_{m,t+1}^{\frac{5}{3}} L_m\right), \quad (5)$$

where

f_m is the fall in the water surface of the river,
H_m is the ponding depth,
Z_m is the land-surface elevation,
L_m is the distance to the river node measured from the downstream end of the river system (fig. 4), and
$\Gamma_{m,t+1}$ is a flow depth the definition of which is a function of flow conditions, as explained subsequently.

The subscript, m, represents a river-system node and its associated river segment. Each of the river nodes corresponds to one of the i,j cell nodes in the 41- by 80-node grid. M is the total number of nodes in a river system. The roughness term, n_m, is computed as $n_m = a\Gamma_m^b$, where a and b are constants associated with a river system. These constants are part of the NSM input data and are a=3.0 and b=0. These values result in n=3.0. The fall is computed at each node as

$$f_m = F_r\left(1 - \frac{(L_r - L_m)}{L_r}\right), \quad (6)$$

where F_r is the change in water-surface elevation over the entire river system, and L_r is the total length of the river system. F_r is constant with time for a river system and is defined in the input data.

If $[(H_{m,t} + Z_m) - (Y_{t+1} + f_m)]$ is less than zero (flow out of the river into the overland system), then Γ_m is an area-weighted flow depth, or

$$\Gamma_{m,t+1} = [a_m(Y_{t+1} + f_m - Z_m) + H_{m,t}(\Delta x \Delta y - a_m)] \div (\Delta x \Delta y), \quad (7)$$

where a_m is the surface area of the river associated with the m river node. If $[(H_{m,t} + Z_m) - (Y_{t+1} + f_m)]$ is greater than zero (flow into the river from the overland system), then Γ_m is equal to the ponding depth in the grid cell associated with that river segment, or

$$\Gamma_{m,t+1} = H_{m,t}. \quad (8)$$

Flow out of the overland system into the river is limited to be less than or equal to the available water volume in the cell above the detention depth, or

$$Q_f \le (H_m - \delta_m)\Delta x \Delta y, \quad (9)$$

where δ_m is the detention (or surface storage) depth and is defined in the input data set as a function of land-use type. However, no limit is placed on the flow out of the river into the overland system, on seepage from the river to the ground-water system, or on evaporation from the river system. This means that, as presently configured in the NSM, the solution of equation 4 does not guarantee mass conservation. Tests were not conducted to determine if mass conservation was actually violated during application of the NSM. Most of the water in the NSM domain is not in the river systems, but in the overland-flow and ground-water systems. Consequently, the failure to ensure mass conservation in the NSM river system probably has little effect on the simulation of water levels and hydroperiod in the Everglades region of the NSM domain.

The flow between the river and ground-water system, or seepage, is computed as

$$R_r = 1.4 \sum_{m=1}^{M} K_m(Y_{t+1} + f_m - h_{m,t})a_{i,j}, \quad (10)$$

where M is the total number of river nodes in a river system, h_m is the ground-water elevation at the m river node, 1.4 is an adjustment to $a_{i,j}$, which is the surface area of the river at node i,j, and K_m is a river seepage coefficient, in feet per day per foot of head, for the m river node that is defined in the input data.

The flow into and out of the river system for each computational time step is determined from an inflow value supplied by the input data and an outflow value

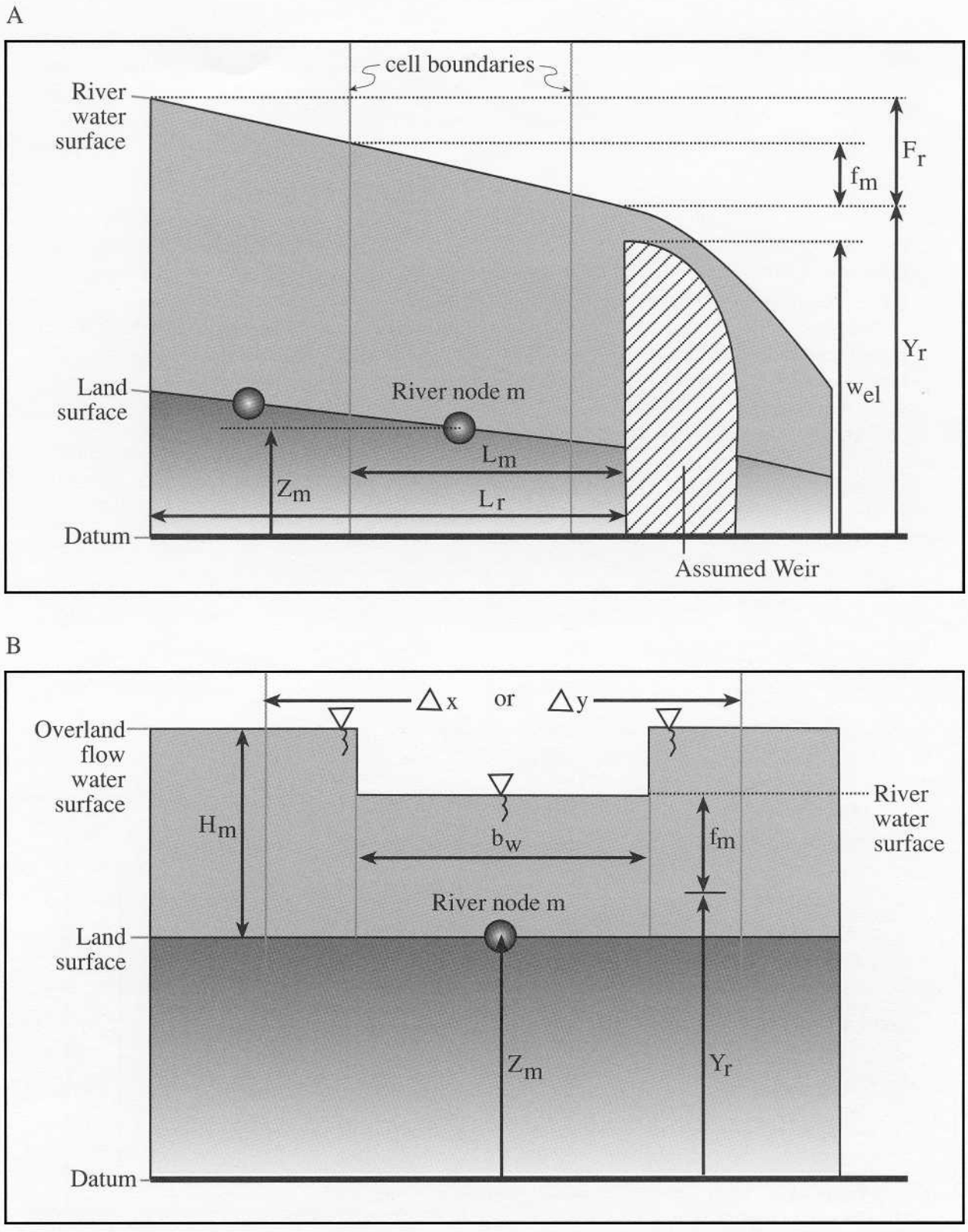

Figure 4. Variables used in the river-system equation. *(A)* Longitudinal view along the length of a river system, and *(B)* Side view of a cell within a river segment.

computed using a weir equation. The resulting equation is

$$Q_r = k_w b_w (Y_{t+1} - w_{el})[2g(Y_{t+1} - w_{el})]^{\frac{1}{2}} \quad (11)$$

$$- q_{t+1},$$

where

k_w is a weir coefficient,
g is the acceleration of gravity,
q_{t+1} is the river-system inflow specified in the input data set at the $t+1$ time step,
b_w is the width of the weir, and
w_{el} is the elevation of the weir crest.

Both b_w and w_{el} are estimates for each river system and are defined as part of the input data.

Evapotranspiration from the river system is computed as

$$E_r = \sum_{m=1}^{M} Emax_m e_m, \quad (12)$$

where $Emax_m$ is the maximum evapotranspiration coefficient which is specified in the input data as a function of land-use type. e_m is the potential evaporation computed for each node from input values of zone potential evapotranspiration, adjusted by input node station weights.

Overland Flow

The overland-flow system is simulated by using a simplified two-dimensional flow equation. The governing equation, numerical solution of the equation, and boundary conditions applied in the solution of the equation are presented in this section.

Equations

The NSM uses a simplified two-dimensional flow equation to represent overland flow. The basic overland-flow equation for each cell is the conservation of mass (fig. 5):

$$A_o \frac{\partial H}{\partial t} = -I_o - E_o + Q_f + P_o + Q_{gw} - Q_o, \quad (13)$$

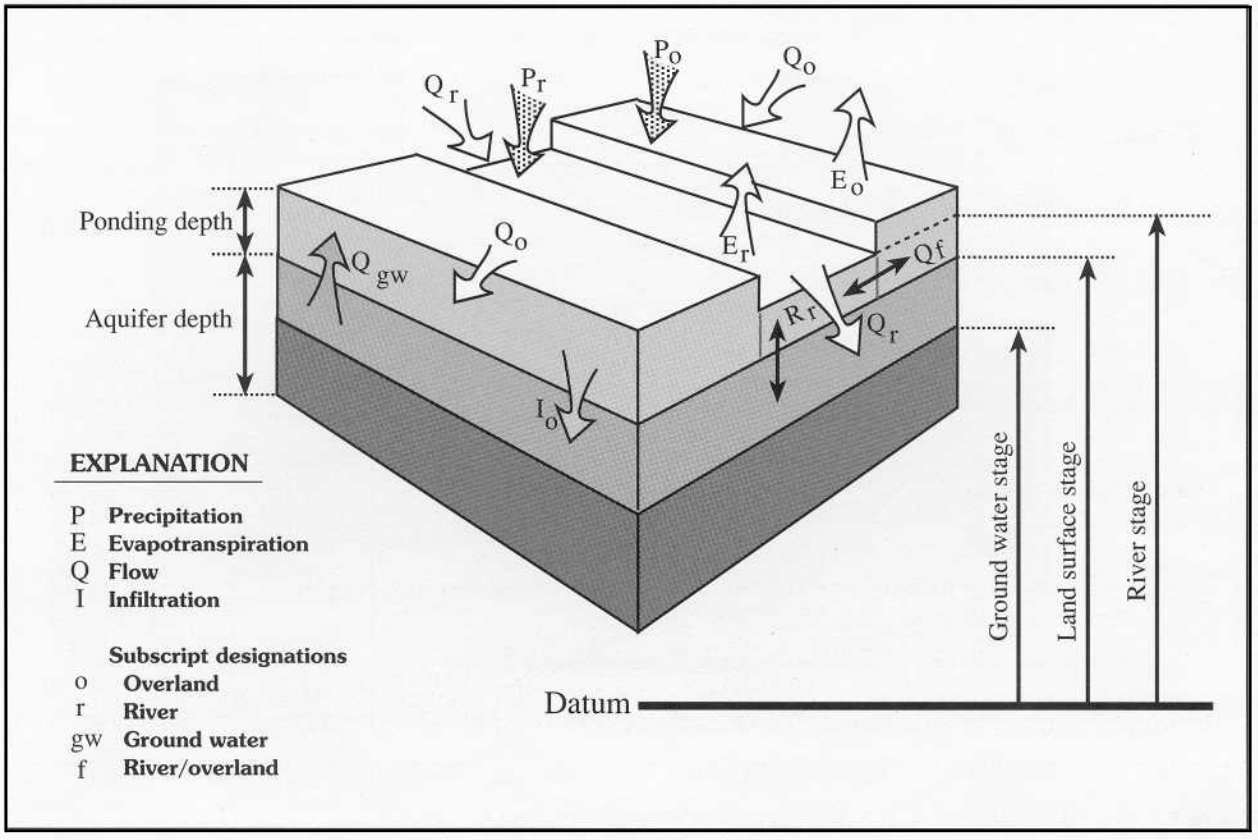

Figure 5. Intracell and intercell hydrologic processes represented within the Natural System Model.

where

I_o is infiltration to the ground-water system,

E_o is the evapotranspiration from the overland-flow system,

H is the water depth (or ponding depth),

Q_f is the flow between the river and overland systems,

P_o is the precipitation,

Q_{gw} is the flow from the ground-water system to the overland system,

and Q_o is the exchange of overland flow between cells.

Although the overland-flow system includes the effects of precipitation, flow between the river and overland system (fig. 6), and flow from the ground-water system, these processes are not explicitly computed in the equations solved for overland flow. Only the exchange of overland flow between cells, infiltration, and evapotranspiration are explicitly computed. Precipitation is added to all ponding depths at the beginning of a time step. The exchange of flow between overland and river systems is simulated during the river-system computations (eq. 5), and flow from the ground-water system is simulated as part of the ground-water equations. Thus, the equation used is

$$\frac{\partial H}{\partial t} + \frac{\partial Hu}{\partial x} + \frac{\partial Hv}{\partial y} = -I_o - E_o, \qquad (14)$$

where the overland flow between cells is represented by the second and third terms on the left side of the equation, u is the overland-flow velocity in the x-direction, and v is the overland-flow velocity in the y-direction.

This equation is discretized by using a simple forward difference in time. Infiltration and evapotranspiration are computed in two separate steps after the computation of overland flow between cells. The technique used to solve the equation is similar to storage routing techniques described by Linsley and others (1975) for one-dimensional flow systems, but is applied to a two-dimensional system in the NSM.

The NSM solves for the exchange of water volumes by overland flow through two of the four sides

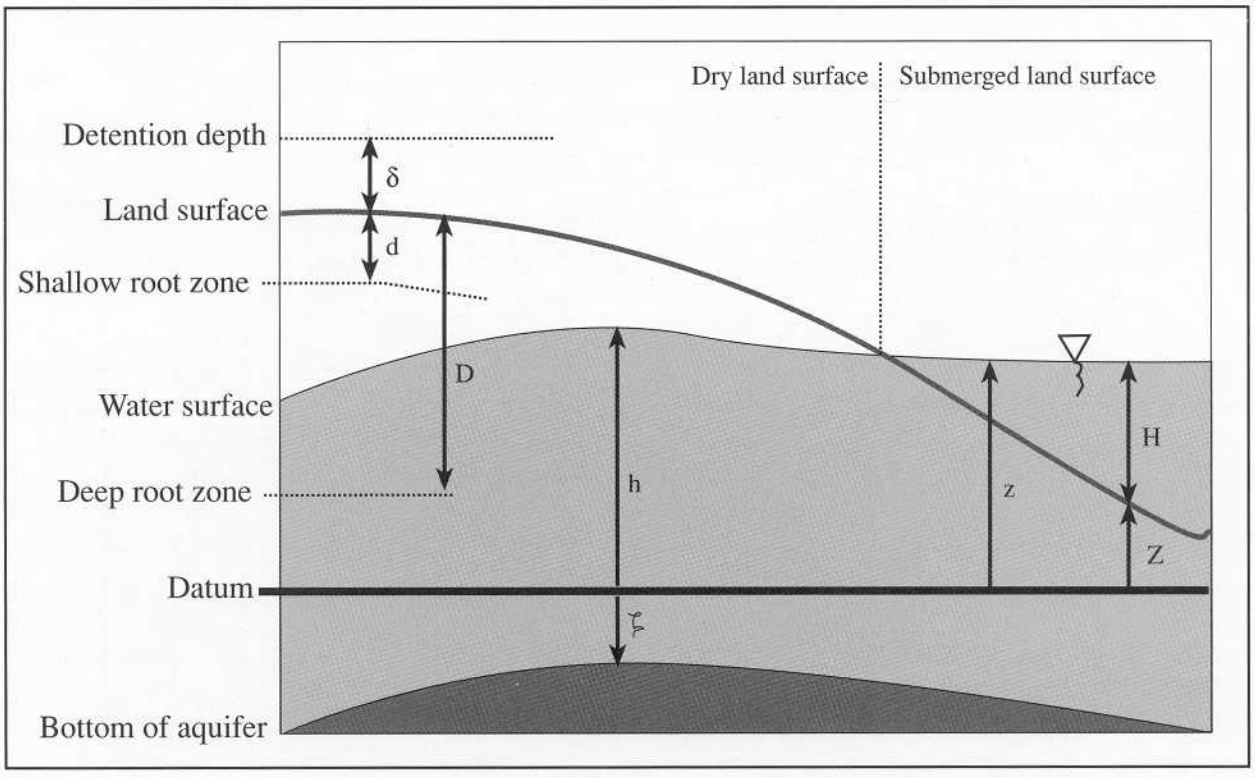

Figure 6. Overland and ground-water flow variables in the Natural System Model.

of a computational cell. The grid is solved in alternating directions (east to west and south to north, and west to east and north to south) to improve solution convergence and to minimize possible solution bias that may occur if the solution proceeded in the same direction for each time step. Information from the current cell (the one for which a solution is desired) and from two adjacent cells, either the cells to the east and south, or the cells to the north and west of the current cell, is used to solve the equations. Mass is balanced over the three cells represented by the three nodes that are used to compute flow through the two cell sides. Ponding depths are computed for the current node at the new time step and are updated with intermediate values at the two adjacent nodes used in computing depth at the current node. This results in two iterations for the solution at a node, one when the node is not the current node and the other when it is.

The numerical method used in the solution of the overland-flow equation is asymmetric and explicit. This results in two equations that are solved for ponding depth, with one equation used for each computational direction. For a computation proceeding from west to east and north to south across the grid (fig. 7A), equation 14 is discretized and solved for ponding depths at the current node at the new time step as

$$H_{i,j,t+1} = H_{i,j,t} - \left[u_{i+\frac{1}{2},j,t+1} H_{i+\frac{1}{2},j,t} \left(\frac{\Delta t}{\Delta x} \right) \right] \quad (15)$$

$$- \left[v_{i,j-\frac{1}{2},t+1} H_{i,j-\frac{1}{2},t+1} \left(\frac{\Delta t}{\Delta y} \right) \right].$$

The ponding depths at the two adjacent nodes are updated with intermediate values as

$$H_{i+1,j,t^*} = H_{i+1,j,t} + u_{i+\frac{1}{2},j,t} H_{i+\frac{1}{2},j,t} \left(\frac{\Delta t}{\Delta x} \right) \quad (16)$$

and

$$H_{i,j-1,t^*} = H_{i,j-1,t} + v_{i,j-\frac{1}{2},t} H_{i,j-\frac{1}{2},t} \left(\frac{\Delta t}{\Delta y} \right), \quad (17)$$

where t^* denotes an intermediate computation that occurs between t and $t + 1$.

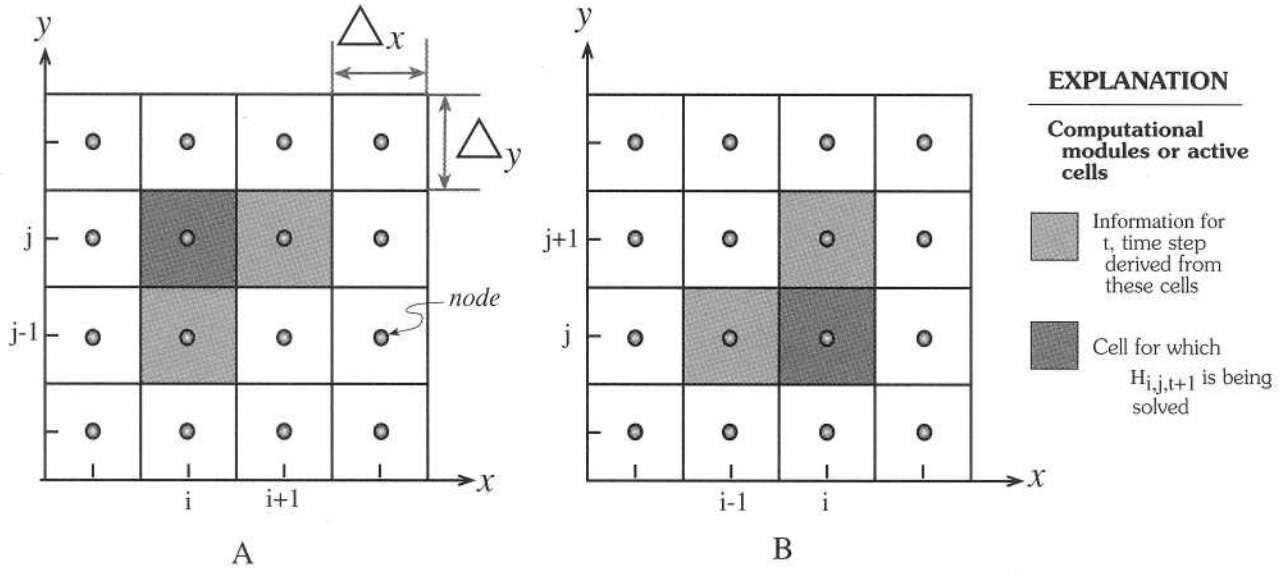

Figure 7. Computational modules or active cells in a grid fragment for solution of overland flow between cells for calculations for $H_{i,j,t+1}$ proceeding from *(A)* west to east and north to south, and *(B)* east to west and south to north.

For east to west and south to north computations across the model grid (fig. 7B), the equation for the current node at the new time step is

$$H_{i,j,t+1} = H_{i,j,t} - \left[u_{i-\frac{1}{2},j,t+1} H_{i,j-\frac{1}{2},t} \left(\frac{\Delta t}{\Delta x} \right) \right] \quad (18)$$

$$- \left[v_{i,j+\frac{1}{2},t+1} H_{i,j+\frac{1}{2},t} \left(\frac{\Delta t}{\Delta y} \right) \right] .$$

For the intermediate ponding depths at the adjacent nodes, the equations used are

$$H_{i-1,j,t^*} = H_{i-1,j,t} + u_{i-\frac{1}{2},j,t} H_{i-\frac{1}{2},j,t} \left(\frac{\Delta t}{\Delta x} \right) \quad (19)$$

and

$$H_{i,j+1,t^*} = H_{i,j+1,t} + v_{i,j+\frac{1}{2},t} H_{i,j+\frac{1}{2},t} \left(\frac{\Delta t}{\Delta y} \right) . \quad (20)$$

The subscripts i, j denote the location of the computed node in the grid, t is the time step, Δx is the grid spacing in the x-direction, Δy is the grid spacing in the y-direction, and Δt is the time-step size.

Finite difference schemes typically align the computational module so that the unknown node lies in the interior of the grid and the known nodes lie on the grid boundaries. Boundary conditions at the new time step can then be used to solve for the unknown node at the new time step with no intermediate updating between the t and t+1 time step. The computational modules for equations 5 and 18 (fig. 7) are not aligned with the known values on the boundaries. Instead, the determination of the values at the unknown boundary node at time t+1 is a function of the type of boundary condition which has been established. Values at the adjacent nodes are then updated at an intermediate time step, t^*, by using equations 19 and 20. This intermediate updating allows the boundary conditions to be transmitted into the grid even though the unknown node is also the boundary condition node.

The velocity terms (u and v) in equations 15 and 18 are computed from the uniform flow, or Manning, equation. The form of the Manning equation used in the NSM can be derived from the two-dimensional momentum equation, which describes the forces represented in the NSM overland-flow equation. The two-dimensional depth-averaged equations for conservation of momentum are

$$\frac{\partial (Hu)}{\partial t} + \frac{\partial (Huu)}{\partial x} + \frac{\partial (Huv)}{\partial y} + gH \frac{\partial Z}{\partial x} + \frac{g}{2} \frac{\partial H^2}{\partial x} \quad (21)$$

$$-\Omega H v + \frac{1}{\rho} \left[\tau_{b.x} - \tau_{s.x} - \frac{\partial H \tau_{xx}}{\partial x} - \frac{\partial H \tau_{xy}}{\partial y} \right] = 0$$

and

$$\frac{\partial (Hv)}{\partial t} + \frac{\partial (Hvu)}{\partial x} + \frac{\partial (Hvv)}{\partial y} + gH \frac{\partial Z}{\partial y} + \frac{g}{2} \frac{\partial H^2}{\partial y} \quad (22)$$

$$-\Omega H u + \frac{1}{\rho} \left[\tau_{b.y} - \tau_{s.y} - \frac{\partial H \tau_{yx}}{\partial x} - \frac{\partial H \tau_{yy}}{\partial y} \right] = 0 ,$$

where

g is acceleration of gravity,

Ω is Coriolis parameter,

ρ is water density,

Z *is* land-surface elevation,

$\tau_{b.x}$ and $\tau_{b.y}$ are bed shear stresses acting in the x- and y-directions, respectively,

$\tau_{s.x}$ and $\tau_{s.y}$ are surface shear (wind) stresses acting in the x- and y-directions, respectively,

and τ_{xx}, τ_{xy}, τ_{yx}, and τ_{yy} are shear stresses caused by turbulence.

If the acceleration, momentum fluxes (first three terms on the left of eqs. 21 and 22), Coriolis, wind stress, and turbulence terms are assumed to be negligible, the momentum equations are reduced to

$$gH \frac{\partial Z}{\partial x} + \frac{g}{2} \frac{\partial H^2}{\partial x} + \frac{1}{\rho} \tau_{b.x} = 0 \quad (23)$$

and

$$gH \frac{\partial Z}{\partial y} + \frac{g}{2} \frac{\partial H^2}{\partial y} + \frac{1}{\rho} \tau_{b.y} = 0 . \quad (24)$$

The bed shear-stress terms in equations 23 and 24 can be formulated using the Manning equation to give

$$\tau_{b.x} = \tau_b \cos(\alpha) = gn^2 \rho \frac{u\sqrt{uu + vv}}{cH^{1/3}} \quad (25)$$

and

$$\tau_{b.y} = \tau_b \cos(\beta) = gn^2 \rho \frac{v\sqrt{uu + vv}}{cH^{1/3}}, \quad (26)$$

where

n is Manning coefficient,

c is a constant to maintain proper unit conversion,

α is the flow angle with respect to the x-axis, and

β is the flow angle with respect to the y-axis.

Substituting equations 25 and 26 into equations 23 and 24, respectively, yields

$$H\frac{\partial Z}{\partial x} + H\frac{\partial H}{\partial y} + \frac{1}{\rho}\left[\rho n^2 \frac{(u\sqrt{uu + vv})}{cH^{1/3}}\right] = 0 \quad (27)$$

and

$$H\frac{\partial Z}{\partial y} + H\frac{\partial H}{\partial y} + \frac{1}{\rho}\left[\rho n^2 \frac{(v\sqrt{uu + vv})}{cH^{1/3}}\right] = 0 . \quad (28)$$

Foot-second units are used in the NSM, so $c = 1.49$. Rearranging equations 27 and 28, solving for u and v, and defining $[\partial Z/\partial x + \partial H/\partial x] = \partial z/\partial x$ and $[\partial Z/\partial y + \partial H/\partial y] = \partial z/\partial y$, where z = water-surface elevation when $z > Z$ (land surface is submerged; fig. 6), the forms of the momentum equations solved by the NSM are

$$u = \frac{1.49}{n} H^{\frac{2}{3}} \sqrt{\cos(\alpha)\frac{\partial z}{\partial x}} \quad (29)$$

and

$$v = \frac{1.49}{n} H^{\frac{2}{3}} \sqrt{\cos(\beta)\frac{\partial z}{\partial y}} . \quad (30)$$

The NSM uses water-surface slope to determine the angle of the flow relative to the grid axis. For the computational module represented in figure 7A, the cosine (α) term in equation 29 is computed as

$$\cos(\alpha) = \frac{\left|z_{i,j,t} - z_{i+1,j,t+1}\right|}{\sqrt{(z_{i,j,t} - z_{i+1,j,t+1})^2 + (z_{i,j,t} - z_{i,j-1,t+1})^2}} . \quad (31)$$

The cosine (β) term in equation 30 is the same as cos (α) in equation 31, except that the numerator in equation 31 becomes $\left|z_{i,j,t} - z_{i,j-1,t+1}\right|$.

The simplified momentum equations (eqs. 29 and 30) are solved for computations proceeding from west to east and north to south (fig. 7A) for the current time step, t+1, in the following forms:

$$u_{i,j,t+1} = \frac{1.49}{n_{i,j}}\left(\frac{(H_{i,j,t} + H_{i+1,j,t+1})}{2}\right)^{\frac{2}{3}} \times \left(\sqrt{\frac{\cos(\alpha_t)\left|z_{i,j,t} - z_{i+1,j,t+1}\right|}{\Delta x}}\right) \quad (32)$$

and

$$v_{i,j,t+1} = \frac{1.49}{n_{i,j}}\left(\frac{(H_{i,j,t} + H_{i,j-1,t+1})}{2}\right)^{\frac{2}{3}} \times \left(\sqrt{\frac{\cos(\beta_t)\left|z_{i,j,t} - z_{i,j-1,t+1}\right|}{\Delta y}}\right) . \quad (33)$$

Flow direction for the velocities is determined from the sign of the difference terms enclosed in the absolute value signs in equations 32 and 33. A set of equations analogous to equations 32 and 33 is solved for computations proceeding from east to west and south to north (fig. 7B).

The Manning coefficient used in equations 32 and 33 (and for the analogous equations for computations proceeding in the east to west and south

to north directions) is for the i,j node. The coefficient is computed from $n_{i,j} = aH_{i,j,t}^{\ b}$, where a and b are constants associated with a land-use type in the i,j node; these constants are part of the input data, with $0.04 < a < 1.45$. Superscript b may be either -0.77 (resistance increases with decreasing flow depth) or 0 (resistance is constant with depth). Yet, velocities are computed from information in the adjacent nodes as well as in the i,j node (eqs. 32 and 33; fig. 7). Consequently, the n-value used to compute the velocities would be more representative of the average roughness along the flow path if a length-weighted coefficient was computed from the roughness in the same nodes as those used in the velocity computation. The use of length-weighted n-values would also ensure that consistent n-values are used in the computations, regardless of the computational direction. Only velocities in nodes which are at the interface of land-use types would be directly affected by this algorithm change, although the effects of these changes would propagate throughout the entire model domain.

Simulation results from explicit numerical methods, such as the method used in the NSM to solve the overland-flow equations, are sensitive to the size of the computational time step. Numerical instabilities can occur in the solution of the overland-flow equation if the simulated velocity in a particular computational cell exceeds the ratio of the grid spacing to the time step. These instabilities occur because the computations propagate flow through more than one computational cell in a single computational time step. The NSM includes an algorithm to maintain numerical stability, by limiting the volume of water that can pass from one cell node in a single computational time step to

$$u\Delta t\Delta x\left(\frac{H_{i+1,j,t} + H_{i,j,t}}{2}\right) \leq \Delta x\Delta x\left(\frac{(z_{i+1,j,t} - z_{i,j,t})}{2}\right). \quad (34)$$

A similar limiting function exists for the y-direction. This limiting function, however, affects the proper selection of the computational time and space step because equation 34 limits the maximum water velocity that can occur in the grid.

Infiltration and evapotranspiration are computed after the exchange of overland flow between cells is computed. The infiltration term, $I_{i,j,t+1}$, is computed when the ponding depth at a node is greater than zero ($H_{i,j,t} > 0$) as

$$I_{i,j,t+1} = S_s(z_{i,j,t} - h_{i,j,t}), \quad (35)$$

where S_s is the input soil storage coefficient and $h_{i,j,t}$ is the elevation of the ground-water surface, which is limited to be less than or equal to the land-surface elevation (see following section). Infiltration is limited to be less than or equal to the ponding depth ($I_{i,j,t} \leq H_{i,j,t}$). Infiltration is added to the recharge term, R_{gw}, of the ground-water flow equation and is subtracted from the ponding depth.

The overland-flow system evapotranspiration, E_o, is dependent on land-use type, ponding depth, and the ground-water elevation at the node. For nodes that have ponding depths greater than the open-water ponding depth, $O_{i,j}$ (or $H_{i,j,t} > O_{i,j}$), E_o is computed in a similar manner as for the river system (eq. 12). Evapotranspiration is computed for nodes having ponding depths less than the open-water ponding depth ($H_{i,j,t} < O_{i,j}$) as

$$E_{i,j,t+1} = \left[(Emax_{i,j} - k_{i,j,t+1})\left(\frac{H_{i,j,t}}{O_{i,j}}\right) + k_{i,j,t+1}\right]e_{i,j}, \quad (36)$$

where k is a daily evapotranspiration coefficient that is interpolated from mid-month values. Both O and k are estimated values that are functions of land-use type and included as part of the input data set.

Evapotranspiration for dry nodes is computed as a function of depth to the ground-water surface. If the depth to ground water is greater than the depth to the deep root zone, $D_{i,j}$, (or $h_{i,j,t} < D_{i,j}$; fig. 6) then $E_o = 0$. If the depth to ground water is greater than the depth to the shallow root zone, $d_{i,j}$, and less than that to the deep root zone (or $D_{i,j} \leq h_{i,j,t} \leq d_{i,j}$; fig. 6), E_o is computed as

$$E_{i,j,t+1} = k_{i,j,t+1}e_{i,j}. \quad (37)$$

$D_{i,j}$ and $d_{i,j}$ are input values and vary with vegetation type. If the depth to ground water is less than the shallow root zone (or $d_{i,j} < h_{i,j,t} \leq Z_{i,j}$; fig. 6), E_o is

$$E_{i,j,t+1} = k_{i,j,t+1}e_{i,j}\frac{(D_{i,j} - (Z_{i,j} - h_{i,j,t}))}{(D_{i,j} - d_{i,j})}. \quad (38)$$

Finally, the evapotranspiration is subtracted from the ponding depth. If the evapotranspiration exceeds the available water for a node, the excess evapotranspiration is subtracted from the recharge term in the ground-water flow equation. Evapotranspiration is not limited when subtracted from recharge, so it is theoretically possible for recharge to become negative.

Boundary Conditions

Overland flow boundary types are no flow, tidal stage, and a water slope. Boundary location and type are determined by logical statements in the source code of the NSM program and cannot be changed by altering the input data file.

No-flow boundary conditions are used by default at grid boundaries when no boundary conditions are explicitly set by program statements and input data. Boundary water-surface elevations are not explicitly set at most of the northern and western boundaries of the grid. Consequently, at these nodes where boundaries are not specified, initial conditions and the depths calculated at the previous time step are used as the boundary water-surface elevations.

The tidal stage boundary condition is used along the Atlantic coast boundary and is

$$H_{i,\,j,\,t+1} = Z_{\text{tide}_{t+1}} - Z_{i,\,j}, \tag{39}$$

where Z_{tide} is the water-surface elevation due to tide. Tidal stages are computed for each node by using mean monthly tidal stages that were measured at selected boundary nodes. Values for other nodes are then computed by linearly interpolating in space and time from the nodes with measured tidal data.

The water slope boundary condition is used along the southwestern edge of the model grid, at the boundary between the ENP and the Gulf of Mexico (fig. 1). This boundary condition is similar to the commonly used normal depth condition. For solutions proceeding from west to east and north to south (fig. 7A), this boundary is expressed as

$$H_{i,\,j,\,t+1} = \frac{1}{2}(H_{i,\,j-1,\,t} + H_{i+1,\,j,\,t}) \tag{40}$$

when

$$\frac{1}{2}(Z_{i,\,j-1,\,t} + Z_{i+1,\,j,\,t}) > Z_{i,\,j,\,t}\,.$$

Otherwise, $H_{i,j,t+1} = \delta_{i,j}$, where $\delta_{i,j}$ is the detention depth. If no node exists at j-1, $H_{i,j,t+1} = H_{i+1,j,t}$. For the solutions proceeding from east to west, south to north the boundary is expressed as

$$H_{i,\,j,\,t+1} = \frac{1}{2}(H_{i,\,j+1,\,t} + H_{i+1,\,j,\,t}) \tag{41}$$

when

$$\frac{1}{2}(Z_{i,\,j+1,\,t} + Z_{i+1,\,j,\,t}) > Z_{i,\,j,\,t}\,.$$

Otherwise, $H_{i,j,t+1} = \delta_{i,j}$. If no node exists at j+1, then $H_{i,j,t+1} = H_{i+1,j,t}$.

Ground-Water Flow

The two-dimensional equation for unconfined ground-water flow is solved to simulate ground-water flow in the NSM. The numerical solution of this equation, along with applied boundary conditions, are presented in this section.

Equations

The ground-water system equation is solved after the overland-flow equations. The two-dimensional equation for unconfined ground-water flow is

$$\frac{\partial}{\partial x}\left(T_{xx}\frac{\partial h}{\partial x}\right) + \frac{\partial}{\partial y}\left(T_{yy}\frac{\partial h}{\partial y}\right) = S\frac{\partial h}{\partial t} + R_{gw}\,, \tag{42}$$

where

T_{xx} *and* T_{yy} are the aquifer transmissivities (units of length squared per time),

S is the storage coefficient,

h is the ground-water elevation, and

R_{gw} is the recharge (units of length per time).

Transmissivity is defined as $T = (h+\zeta)*\kappa$, where ζ is the aquifer depth measured from a common datum (fig. 6), and κ is the hydraulic conductivity (units of length per time).

Equation 42 is a diffusion-type equation and is solved explicitly at new time steps for h, the ground-water elevation, in the NSM by using a finite-difference formulation which is forward in time and central in space. This technique is an asymmetric numerical approximation that was introduced by